Performance Analysis for Optical OFDM Transmission in Short-Range IM/DD Systems

Liang Chen, Brian Krongold, and Jamie Evans

***Abstract*—This paper investigates the performance of some recently proposed optical orthogonal frequency-division multiplexing (OFDM) transmission techniques in a short-range intensity-modulated, direct-detected (IM/DD) optical channel. Due to the unipolarity of the IM/DD channel, asymmetric clipping and associated nonlinear distortion is inevitable, resulting in an unfavorable dc power and a significant performance penalty. Using a detailed analysis of the clipped signal, our recent work focused on reducing this clipping-resulted dc via both power optimization and frequency planning. In this paper, a set of effective receiver signal-to-noise ratio formulas is proposed, which helps in accurately and efficiently evaluating the system performance across various optical OFDM systems. We conduct a power efficiency analysis to reveal tradeoffs between power and spectral efficiencies among different systems. Our results show that with a cost of additional complexity, a diversity-combining technique offers significant benefits in all cases.**

***Index Terms*—Direct detection, intensity modulation, optical orthogonal frequency-division multiplexing (OFDM).**

I. Introduction

RECENTLY, as one of the promising solutions to combat signal dispersion, optical orthogonal frequency-division multiplexing (OFDM) systems have gained a strong interest in both academic and industrial sectors due to its scalability with data rate and/or transmission distance. Consequently, different flavors of optical OFDM systems have been proposed in either short-range free space [1]–[3], multimode fiber (MMF) [4]–[9], plastic optical fiber (POF) [10]–[12], or long-haul single-mode fiber (SMF) systems [13]–[19].

An optical OFDM system, where the aggregate throughput is distributed over a large set of partially overlapped yet orthogonal subchannels, is able to improve the immunity to turbulence and nonlinearities, as well as the tolerance to both chromatic [6] and polarization-mode dispersion [20]. Instead of trying to compensate the dispersion completely, optical OFDM intrinsically reduces the baud rate and, consequently, the amount of accumulated dispersion penalty. Moreover, with a proper choice of cyclic prefix, optical OFDM signals have the ability of greatly alleviating or even completely eliminating the dispersion penalty.

As a result of the nonlinear photodetection process, the performance of long-haul SMF systems is limited by chromatic as well as polarization-mode dispersion. In these scenarios, optical single-sideband OFDM modulation [13] or OFDM systems with coherent optical transceivers [15], [17] have demonstrated the ability to fully compensate the dispersion by providing a one-to-one frequency mapping between optical and electronic domains. While in short-range, free-space, POF or MMF systems, which is the focus of this paper, the achievable rate is largely limited by a combination of optical power and modal dispersion. A better alternative is to employ noncoherent OFDM transmission directly onto existing intensity-modulated, direct-detected (IM/DD) transceivers as it requires minimal modifications and, hence, is very attractive for its compactness and cost-effectiveness.

Due to incompatibility between the unipolar IM/DD optical channel and bipolar electronic OFDM signalling, conventional OFDM systems cannot be employed without modification. Furthermore, as the instantaneous envelope of the OFDM waveform generally follows a Gaussian distribution with a large peak-to-average power ratio, the OFDM signal is very sensitive to nonlinear effects. To overcome the nonlinear distortion due to clipping of negative peaks, IM/DD optical OFDM transmission requires either an additional electronic bias [2]–[4], or an odd-subchannel-only bit-loading pattern [21]. Recent research [22]–[24] shows that for short-range transmission, there is a tradeoff between spectral and power efficiencies. Some previous work has indeed been focused on using both distortion-less and distortion-introducing techniques to improve this power-spectrum tradeoff [6]–[8], [25]–[29]. In this paper, we provide an extended comparison of both electronic and optical power efficiencies for various IM/DD optical OFDM systems.

The rest of this paper is organized as follows: the system model of a short-range IM/DD optical OFDM system is presented in the next section. In Section III, we provide an overview of various IM/DD optical OFDM transmission schemes and focus on the representations of their electronic and optical power. The effective receiver SNR and bit error rate (BER) performance are characterized through both theoretical analysis and simulation in Section IV. Simulation results and discussions about the system power efficiency are presented in Section V before we draw conclusions.

Manuscript received July 11, 2011; revised December 23, 2011; accepted January 10, 2012. Date of publication February 03, 2012; date of current version February 24, 2012.

The authors are with National ICT Australia, Victoria Research Laboratory, Department of Electrical and Electronic Engineering, School of Engineering, University of Melbourne, Parkville, Vic. 3010, Australia (e-mail: lianchen@ee.unimelb.edu.au; bsk@ee.unimelb.edu.au; jse@ee.unimelb.edu.au).

Color versions of one or more of the figures in this paper are available online at http://ieeexplore.ieee.org.

Digital Object Identifier 10.1109/JLT.2012.2185779

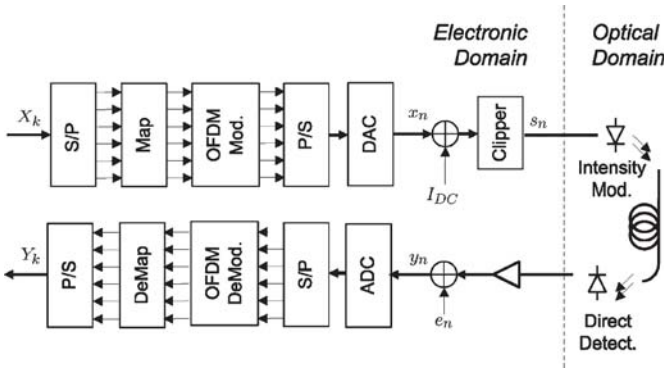

Fig. 1. Short-range IM/DD optical OFDM system model.

II. System Description

An example of a short-range IM/DD optical OFDM system considered here is shown in Fig. 1. At the transmitter, incoming high-speed data are first split into a large number of low-speed datasets by a serial-to-parallel converter before being encoded into quadratic-amplitude modulation (QAM) symbols and applied onto N equally spaced subchannels. The complex symbols are then transformed into a time-domain signal via an inverse fast Fourier transform (IFFT). The n-th sample of the output is given by

$$x_n = \frac{1}{N}\sum_{k=0}^{N-1}\left(X_k^I + jX_k^Q\right)\exp\left(j\frac{2\pi}{N}kn\right) \tag{1}$$

where $X_k^I + jX_k^Q$ is the complex symbol modulated on the k-th subchannel. In order to focus on nonlinear clipping effects, we will look at the case where a real-valued signal is produced. Therefore, as in the case of digital multitone modulation [30], we enforce conjugate symmetry by setting $X_k^I = X_{N-k}^I$ and $X_k^Q = -X_{N-k}^Q$ for all $k < N/2$ except the first one. For the case of complex output, an intermediate frequency can be inserted to generate real waveforms via electronic I/Q modulation [13].

As the OFDM signal is the sum of a group of independent, identically distributed components, for any practical choice of subchannel number and/or alphabet size, x_n becomes approximately Gaussian due to the central limit theorem. In the case of a real output, as a result of conjugate symmetric bit-loading, some correlation can be observed among x_n sequences. However, with a large subchannel number, $\{x_n\}$ can still be well approximated as i.i.d. Gaussian random variables [31]. Fig. 2 shows the time-domain characteristics of a simulated OFDM system with only 16 subchannels, each loaded with 4-QAM symbols. The output time-domain signal is first normalized so that the empirical variance is equal to one. Its probability density function (pdf) and cumulative distribution function (cdf) are then evaluated. The results suggest that we can accurately model the x_n sequence using an independent identically distributed Gaussian process with the following pdf:

$$p_x(x) = \mathcal{N}\left(x; 0, \mathrm{E}\left[|X_k|^2\right]\right) \tag{2}$$

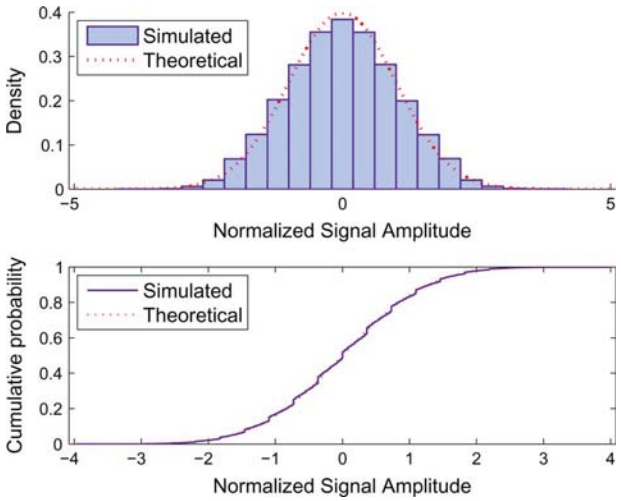

Fig. 2. Approximately Gaussian distributed time-domain OFDM Signal.

where

$$\mathcal{N}(x;\mu,\sigma^2)\triangleq\frac{1}{\sqrt{2\pi}\sigma}e^{-\frac{(x-\mu)^2}{2\sigma^2}} \tag{3}$$

is a standard Gaussian distribution function with mean μ and variance σ^2.

Depending on the details of the OFDM modulator, not all subchannels need be loaded and/or the output x_n sequence may have been shaped/combined to form some useful properties (e.g., with certain bit-loading patterns across subchannels [21], [26], [29], strong correlations can be observed among IFFT output samples). However, by slightly modifying the above model and including only the independent samples, the overall analysis presented in this paper remains valid.

The output of the OFDM modulator is then transformed into a digital data sequence via a parallel-to-serial converter. A digital-to-analog converter (DAC) is used to convert this sequence into an analog waveform, which is generally bipolar. A biasing and clipping process can then be employed so this signal can be delivered by a unipolar IM/DD system. If we denote the biasing voltage by I_{DC}, the asymmetrically clipped time-domain samples s_n, which represents the output distorted signal sequence are

$$s_n = \begin{cases} 0, & x_n < -I_{\mathrm{DC}} \\ x_n + I_{\mathrm{DC}}, & x_n \geq -I_{\mathrm{DC}}. \end{cases} \tag{4}$$

This helps us to avoid the complexity and high cost associated with an analog clipping device. In general, although the analog driving signal may still dip below 0 due to DAC and filtering, the effect is negligible [32].

This unipolar signal is then used to drive a linear optical modulator. For simplicity, we assume an ideal intensity modulator is used here, where the instantaneous output optical power is a replica of the corresponding electrical-drive signal.[1] The output optical beam will then travel through a channel suffering from various attenuations, dispersions and nonlinear effects before the distorted signal hits the receiver where it may again be corrupted by electronic noise. A cyclic prefix can be added to each

[1]For a more detailed analysis about modulator nonlinearities, see [32].

OFDM symbols so that both the inter-symbol interference and inter-channel interference due to delay spread/modal dispersion can be eliminated.

For short-range applications, the achievable rates are limited by a combination of both optical power and modal dispersion. Thus, even though IM/DD optical OFDM can only compensate the linear impairments, it is reasonable to start with a simple case where loss and dispersion are fully compensated. The system performance is then limited by the receiver electronic noise, and the optical channel is, therefore, modeled as an additive white Gaussian noise (AWGN) vector channel. In reality, some of the optical noise is related to the transmit optical power and consequently has a strong correlation with the time-domain signal. In OFDM systems, however, this power dependence can be greatly alleviated due to its frequency-domain parallel transmission, where the noise power is spread over the entire spectrum through the demodulating FFT process. We assume appropriate algorithms can be performed at the OFDM receiver to recover the information.

III. Statistical Characterization of the Clipped Signal

The information is modulated onto the electronic signal s_n in the form of either current or voltage with its electronic power $\mathbf{P}_e$ proportional to $\mathrm{E}[s_n^2]$. On the other hand, the intensity modulator generates a beam with its optical intensity/power $\mathbf{P}_o$ proportional to $\mathrm{E}[s_n]$. Without loss of generality, we define $\mathbf{P}_e = \mathrm{E}[s_n^2]$ and $\mathbf{P}_o = \mathrm{E}[s_n]$ as in [23]. The power ratio $\mathbf{P}_o/\mathbf{P}_e$ then indicates the transmission efficiency which determines the amount of actual energy required to achieve a desired signal strength after the photodetector. This serves as a starting point for our power efficiency analysis. We note that the electronic-optical power relationship can differ from one system to another and is indeed dependent on the statistics of the s_n sequence. Hence, in this section, we give a brief summary of the IM/DD optical OFDM transmission with a focus of theoretical characterization of the electronic and optical power of the clipped signal, s_n. We consider both the case of 1) dc-biased OFDM systems where additional electronic biases are used; as well as 2) asymmetrically clipped OFDM where certain bit-loading patterns are used to avoid the additional biasing.

A. DC-Biased OFDM

1) Sufficiently Biased OFDM: Many previous works have assumed an *appropriate* and variable dc offset is added [3], [5], [10]. Depending on the minimum value of the IFFT output samples, I_{DC} is chosen on a symbol-by-symbol basis to avoid clipping. The output power is simply

$$\mathrm{E}[s_n] = I_{\mathrm{DC}}, \quad \mathrm{E}\left[s_n^2\right] = \sigma^2 + I_{\mathrm{DC}}^2 \tag{5}$$

where $\sigma^2 = \mathrm{E}[|X_k|^2]$ is the transmitted average electronic energy per QAM symbol.

2) Fixed-Biased OFDM: To improve power efficiency, other works [2], [6], [11], [12], [22], [23] have used *fixed*, yet large enough power, to ensure an infrequent clipping from a statistical point of view. In the low-bias region, since a significant amount of power will be clipped out, the pdf of the transmitted signal s_n is

$$p_s(x) = \begin{cases} \mathcal{N}(x; I_{\mathrm{DC}}, \sigma^2), & x > 0 \\ Q\left(\dfrac{I_{\mathrm{DC}}}{\sigma}\right)\delta(x), & x = 0 \end{cases} \tag{6}$$

where $\delta(x)$ is the Dirac delta function with a unit impulse at x only and the well-known Q-function is defined as the integral over normal pdf

$$Q(\nu) \triangleq \int_{\nu}^{\infty} \mathcal{N}(\tau; 0, 1) d\tau \triangleq 1 - \Phi(\nu). \tag{7}$$

Hence, the transmit power becomes

$$\begin{aligned} \mathrm{E}[s_n] &= \int_{-\infty}^{\infty} x \cdot p_s(x)\, dx \\ &= \frac{\sigma}{\sqrt{2\pi}}\, e^{-\frac{I_{\mathrm{DC}}^2}{2\sigma^2}} + I_{\mathrm{DC}}\, \Phi\left(\frac{I_{\mathrm{DC}}}{\sigma}\right) \end{aligned} \tag{8}$$

$$\begin{aligned} \mathrm{E}\left[s_n^2\right] &= \int_{-\infty}^{\infty} x^2 \cdot p_s(x)\, dx \\ &= \left(\sigma^2 + I_{\mathrm{DC}}^2\right)\, \Phi\left(\frac{I_{\mathrm{DC}}}{\sigma}\right) + \frac{\sigma I_{\mathrm{DC}}}{\sqrt{2\pi}}\, e^{-\frac{I_{\mathrm{DC}}^2}{2\sigma^2}}. \end{aligned} \tag{9}$$

When the bias I_{DC} is large, the aforementioned equations can be well approximated by (5).

3) Optimally Biased OFDM: More recently, searching for an optimal biasing level has been attempted through both simulation and theoretical analysis [7], [8], [24], [32]. In these cases, since the optimal bias strategy is a special case of the fixed bias where the receiver SNR is maximized, (8) and (9) can still be applied.

B. Asymmetrically Clipped OFDM

1) ACO-OFDM: Using only the odd subchannels, ACO-OFDM systems [21] provide a tradeoff between power and spectral efficiency. The x_n sequence of ACO-OFDM is known to be antiperiodic: for any sample point in the first half of an OFDM symbol, there exists another unique sample point in the second half with the same amplitude but opposite sign, i.e., $x_n = -x_{n+(N)/(2)}$. As a result of loading only half of the available subchannels per OFDM symbol, the electronic power is halved, $\mathrm{E}[x_n^2] = \sigma^2/2$. With no additional bias, i.e., $I_{\mathrm{DC}} = 0$ in (4) and (6), all negative samples are replaced by 0's after clipping. Due to the asymmetry, exactly one copy of the original information-conveying data sample pairs is preserved, and the resulting output power is

$$\mathrm{E}[s_n] = \int_0^{\infty} x \cdot \mathcal{N}\left(x; 0, \frac{1}{2}\sigma^2\right)\, dx = \frac{\sigma}{2\sqrt{\pi}} \tag{10}$$

$$\mathrm{E}\left[s_n^2\right] = \int_0^{\infty} x^2 \cdot \mathcal{N}\left(x; 0, \frac{1}{2}\sigma^2\right)\, dx = \frac{1}{4}\sigma^2. \tag{11}$$

Note that the aforementioned equations are also special cases of (8) and (9) with an adjusted $\mathrm{E}[x_n^2]$ and $I_{\mathrm{DC}} = 0$.

2) Asymmetrically Clipped, Diversity-Combined OFDM: When only the odd subchannels are loaded, the clipping distortion, which corresponds to the FFT of the $|x_n|$ sequence,

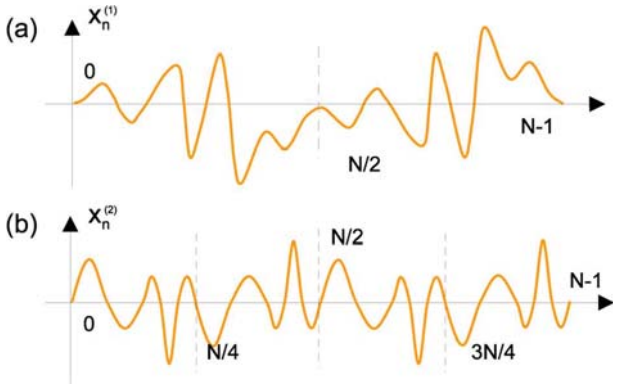

Fig. 3. Example of (a) an antiperiodic waveform and (b) an antiperiodic as well as periodic waveform.

falls exclusively onto the even subchannels [26]. This natural separation of signal and distortion indicates that at the receiver side, some extent of spectral diversity can be observed. Based on this idea, we proposed the asymmetrically clipped, diversity-combined OFDM (AC/DC-OFDM) system in [26]. With the help of one additional IFFT/FFT pair, two separate estimators of x_n are generated and then combined to improve the effective SNR. Since AC/DC-OFDM involves only receiver-side signal processing with no transmitter modifications, the transmit power is exactly the same as defined in (10) and (11), but results in a higher effective received SNR.

3) Asymmetrically Clipped, Successively Decoded OFDM: The spectral diversity presented on an asymmetrically clipped antiperiodic signal can also be converted into higher spectral efficiency. In [29], we extended the idea of using only odd subchannels to an expanded set of particular subchannels combinations. By characterizing and compensating for the clipping distortion, parallel transmission of multiple antiperiodic signals can be achieved. In these asymmetrically clipped, successively decoded OFDM (AC/SD-OFDM) systems, both odd and even subchannels can be loaded with data to create a class of antiperiodic signals. This, in turn, provides a much higher spectral efficiency. These signals $x_n^{(i)}$ are separately clipped, then combined together to form the unipolar driving signal. ACO-OFDM, hence, is a special case of this class where the set of odd subchannels $\{1,\ 3,\ 5, \ldots, N-1\}$ are used for bit loading as shown in Fig. 3(a). Fig. 3(b) shows an example of when an additional subchannel group $\{2,\ 6,\ 10, \ldots, N-2\}$ is loaded, and its IFFT output waveform $x_n^{(2)}$ becomes periodic as well as antiperiodic.

The electronic driving current of AC/SD-OFDM is the superposition of several asymmetrically clipped anti-periodic signals i.e.,

$$s_n = s_n^{(1)} + s_n^{(2)} + \cdots + s_n^{(u)}. \tag{12}$$

Similar as in ACO-OFDM, in order to create an antiperiodic signal $x_n^{(i)}$, only $N/2^i$ of subchannels are loaded with data. As a result, if we denote the variance of $x_n^{(i)}$ by σ_i^2, we have $\sigma_i^2 = \sigma^2/2^{i+1}$.

The exact pdf of s_n is the result of a series of convolutions and is quite messy when u is large. Nevertheless, using the basic property of linearity and independence, the output power can simply be expressed as

$$\mathrm{E}[s_n] = \mathrm{E}\left[s_n^{(1)}\right] + \mathrm{E}\left[s_n^{(2)}\right] \cdots + \mathrm{E}\left[s_n^{(u)}\right] = \sum_{i=1}^{u} \frac{\sigma_i}{\sqrt{\pi}} \tag{13}$$

$$\begin{aligned}\mathrm{E}\left[s_n^2\right] &= \sum_{i=1}^{u} \mathrm{E}\left[s_n^{(i)} s_n^{(i)}\right] + 2\sum_{i=1}^{u-1}\sum_{j=i+1}^{u} \mathrm{E}\left[s_n^{(i)}\right]\mathrm{E}\left[s_n^{(j)}\right] \\ &= \sum_{i=1}^{u} \sigma_i^2 + \sum_{i=1}^{u-1}\sum_{j=i+1}^{u} 2\frac{\sigma_i \sigma_j}{\pi}.\end{aligned} \tag{14}$$

IV. Effective Receiver SNR

As mentioned in Section II, it is valid to start with a simple AWGN vector channel, where the received signal r_n is given by

$$r_n = s_n + e_n \tag{15}$$

and e_n is a zero-mean Gaussian noise process used to denote the joint effect of various noise processes which may be present at the receiver side with a two-side power spectral density of $N_0/2$. The detected signal contains an unfavorable dc component which does not contribute to the receiver SNR. Therefore, in order to fully characterize the power efficiency of a particular system, a theoretical analysis of the effective SNR and BER performances is provided in this section.

In making a fair comparison, we assume that after the receiver's photodetector, the resulting time-domain waveforms for different systems have the same average energy per OFDM symbol E_s. We define the bandwidth of a particular received signal as the first zero crossing on its power spectrum [33]. A N-point IFFT/FFT with no oversampling is used so that when N is large, roughly all modulation schemes would have the same bandwidth. We also normalize this bandwidth to unity for comparison purposes. For OFDM with 2-D constellations, such as QAM, the total noise power is then N_0. In this section, we will focus on finding the BER for each system in terms of the average electronic SNR, E_s/N_0.

A. DC-Biased Optical OFDM

For dc-biased OFDM, since a real output at the transmit IFFT is desired, only half of the subchannels will be loaded with data symbols to form a conjugate symmetry [30]. Furthermore, the additional bias power of I_{DC}^2 makes the output power of s_n much larger than x_n. Since we have limited the OFDM symbol energy to E_s for all different systems, the signal must then pass through an automatic gain control unit to make sure the transmit power remains the same. We further note that this dc bias inside the received waveform will be canceled out after the demodulating FFT operation due to the circular symmetry of the "exp" components [8]. Thus, for a particular OFDM symbol, when the bias is large enough to avoid any clipping distortion, the effective SNR per received QAM symbol is

$$\mathrm{SNR}(\gamma) = \frac{E_s}{N_0} \cdot \frac{E_s}{E_s + I_{\mathrm{DC}}^2} = \frac{E_s}{N_0} \cdot \frac{1}{1+\gamma^2} \tag{16}$$

where $\gamma = I_{\mathrm{DC}}/\sqrt{E_s}$ is defined as the normalized bias.

For moderate to large SNRs and gray-coded assignment, the BER for M-QAM modulation can be approximated as [34]

$$\mathrm{BER} = \frac{4}{\log_2 M}\left(1-\frac{1}{\sqrt{M}}\right) Q\left(\sqrt{\frac{3}{M-1}\mathrm{SNR}}\right). \quad (17)$$

Therefore, in order to evaluate the BER performance, it is sufficient to start with the effective SNR per symbol for different systems.

1) Sufficiently Biased OFDM: When a sufficient biasing strategy is used, the value of γ varies from one OFDM symbol to another, and depends on the minimum value of the IFFT output samples. For systems using an N-point IFFT/FFT, it can be modeled as a random variable with the following cdf:

$$\begin{aligned} P(\Gamma \le \gamma) &= P[\min(x_1, x_2, \ldots, x_N) \ge -\gamma] \\ &= \prod_{n=1}^{N} \Pr(x_n \ge -\gamma) = [\Phi(\gamma)]^N. \end{aligned} \quad (18)$$

The pdf of Γ is then

$$\begin{aligned} P_\gamma &= P(\Gamma = \gamma) = \frac{d\,P(\Gamma \le \gamma)}{d\,\gamma} \\ &= -\Phi'(\gamma)\cdot N[\Phi(\gamma)]^{N-1}. \end{aligned} \quad (19)$$

Since $\Phi(x)$ is the cdf of a standard Gaussian distribution, the derivative of $\Phi(x)$ follows immediately from its definition and the pdf of the biasing level γ can be rewritten as

$$P_\gamma = \frac{N}{\sqrt{2\pi}}\exp\left(-\frac{\gamma^2}{2}\right)[1-Q(\gamma)]^{N-1}. \quad (20)$$

The overall BER for an M-QAM sufficiently biased optical OFDM system can then be evaluated using

$$\mathrm{BER_S} = \int_0^\infty P_\gamma \cdot \mathrm{BER}(\gamma)\, d\gamma \quad (21)$$

where $\mathrm{BER}(\gamma)$ can be obtained by substituting (16) into (17).

Fig. 4(a) shows the pdf of the sufficient bias γ, obtained using (20), for various choices of subchannel numbers. It is easy to conclude that the probability of having γ larger than 5 is extremely small. Consequently, even though a closed form expression of the BER is not available, numerical evaluation of (21) over a limited, yet small range of γ readily provides us with a very good approximation, as shown in Fig. 4(b).

2) Fixed-Biased OFDM: The extremely small probability of requiring a large bias also enables us to use a fixed, rather than a sufficient, bias $\bar{\gamma}$ to achieve higher power efficiency. With a careful choice of this fixed bias, the probability of clipping can be well controlled.

The effect of insufficient biasing and the following clipping process can be accurately modeled into an attenuation on the signal constellation plus an uncorrelated additional clipping noise [8]. The normalized transmit signal is then

$$s_n \approx \frac{K x_n + z_n}{\sqrt{K^2+\bar{\gamma}^2}} \quad (22)$$

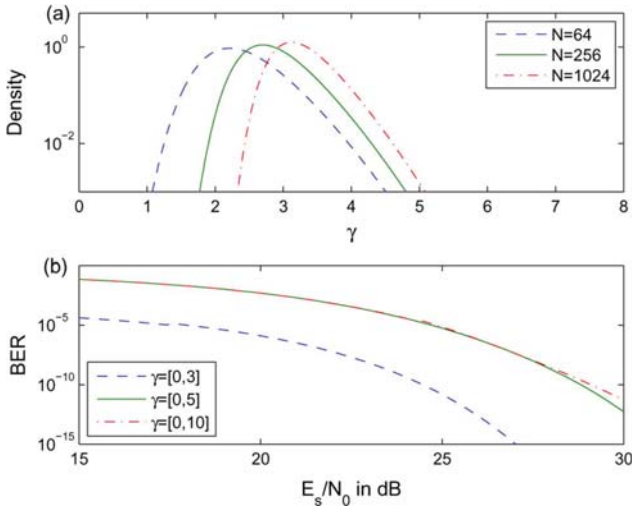

Fig. 4. (a) cdf of γ for different N. (b) BER approximation using different range of γ for $N = 1024$.

where the attenuation factor K and clipping noise power σ_z^2 are both functions of the bias level $\bar{\gamma}$ and can be quantified following our previous work in [8]:

$$K = 1 - Q(\bar{\gamma}) = \Phi(\bar{\gamma}) \quad (23)$$

$$\begin{aligned} \sigma_z^2 = E_s \Big\{ &(1+\bar{\gamma}^2)[Q(\bar{\gamma}) - Q^2(\bar{\gamma})] - \frac{1}{2\pi}e^{-\bar{\gamma}^2} \\ &- \frac{\bar{\gamma}}{\sqrt{2\pi}}e^{-\frac{\bar{\gamma}^2}{2}}[1-2Q(\bar{\gamma})]\Big\}. \end{aligned} \quad (24)$$

This model is shown to give the best linear mean-square error approximation, where the uncorrelated time-domain clipping noise z_n has a bounded pdf. Under our AWGN channel assumption, the detected signal after the OFDM FFT demodulator contains two Gaussian-like noise terms as a result of the central limit theorem [8]. The frequency-domain additive noise attributed from e_n has a variance of N_0, while the frequency-domain additive clipping noise attributed from z_n has a variance of $\sigma_z^2/(1+\gamma^2)$. Therefore, the effective SNR per symbol for a fixed-bias level of $\bar{\gamma}$ is then

$$\mathrm{SNR_F} = \frac{E_s \cdot \frac{K^2}{1+\bar{\gamma}^2}}{\frac{\sigma_z^2}{1+\bar{\gamma}^2} + N_0}. \quad (25)$$

When the fixed bias $\bar{\gamma}$ is very large, K quickly goes to 1 while σ_z^2 approaches zero. The effect of nonlinear clipping distortion is negligible and the aforementioned SNR expression is then reduced to (16).

3) Optimally Biased OFDM: An alternative approach is to further optimize the fixed bias by taking into account the actual system setups and requirements, e.g., modulators with nonlinear transfer functions, ADCs with finite dynamic range and resolutions, channels with fading, and receivers with certain SNR figures. We adopt our previous approach in [8] and denote the transmitted-signal-to-clipping-noise ratio as $\mathrm{SNR}_c = (K^2 E_s)/(\sigma_z^2)$ and the received-signal-to-receiver-noise ratio as

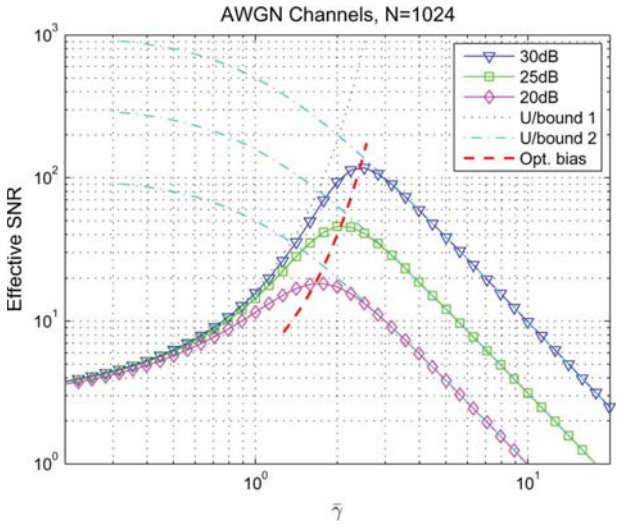

Fig. 5. Effective SNR versus biasing level $\bar{\gamma}$ for different E_s/N_0.

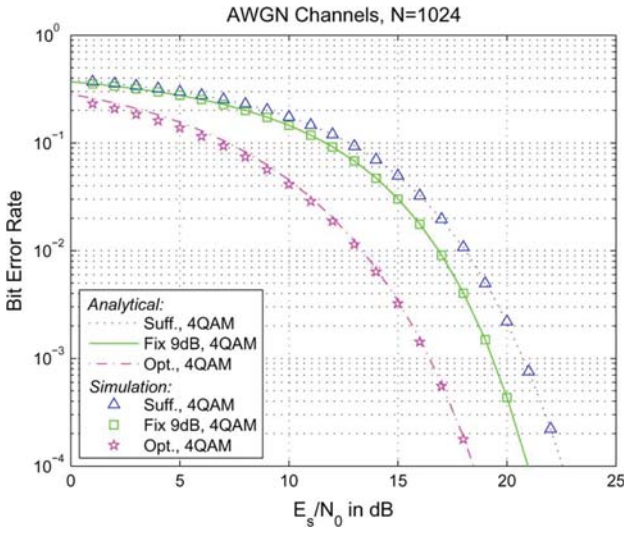

Fig. 6. BER as a function of E_s/N_0 for dc-biased optical OFDM systems.

$\mathrm{SNR}_d = (K^2 E_s + \sigma_z^2)/((1+\gamma^2)N_0)$. After some simple manipulations, the effective receiver SNR in (25) can be consequently rewritten into

$$\mathrm{SNR_P} = \frac{\mathrm{SNR_c}\ \mathrm{SNR_d}}{1 + \mathrm{SNR_c} + \mathrm{SNR_d}}. \tag{26}$$

Note that (26) is not a monotonic function of γ as shown in Fig. 5. In the low-bias region, $\mathrm{SNR}_c \ll \mathrm{SNR}_d$. Hence, by ignoring the effect of receiver noise, the effective SNR is simply bounded by **Upper Bound 1**:

$$\mathrm{SNR_P} = \frac{E_s \cdot \frac{K^2}{1+\gamma^2}}{\frac{\sigma_z^2}{1+\gamma^2} + N_0} \le \frac{E_s \cdot \frac{K^2}{1+\gamma^2}}{\frac{\sigma_z^2}{1+\gamma^2}} = \mathrm{SNR}_c. \tag{27}$$

When increasing the biasing power in this region, SNR_c as well as the total effective SNR begin to increase, thereby leading to a decreased BER.

On the other hand, with a very large biasing power, the effect of clipping distortion is negligible, i.e., $K \approx 1$ and $\sigma_z^2 \approx 0$. Since $\mathrm{SNR}_c \gg \mathrm{SNR}_d$, the effective SNR is also bound by **Upper Bound 2**:

$$\begin{aligned}\mathrm{SNR_P} &= \frac{\mathrm{SNR_d}}{1 + \frac{1+\mathrm{SNR_d}}{\mathrm{SNR_c}}} \le \mathrm{SNR_d} \\ &\le \frac{(1 \cdot E_s - 0)}{N_0(1+\gamma^2)} = \frac{E_s}{N_0} \cdot \frac{1}{1+\gamma^2}.\end{aligned} \tag{28}$$

This bound indicates that with excessive biasing power, the effective SNR starts to decrease since a very large portion of the received signal power is its dc component.

Therefore, for any given dc-biased OFDM system with a specific E_s/N_0 value, there exists an optimal biasing level, γ^*, as shown in Fig. 5. Due to the power normalization, the maximized effective SNR is always smaller than the original E_s/N_0 and is always below the aforementioned Upper Bound 1 and Upper Bound 2. With an increased received SNR, the optimal bias increases as well. By applying the fast searching algorithm in [8], the optimal bias point which maximizes the effective SNR can be readily located.

Fig. 6 shows the analytical and corresponding simulation results for different types of dc-biased optical OFDM systems in a simulated AWGN channel, where 1 000 000 random binary bits are tested in a Monte Carlo setup. All dc-biased OFDM systems present significant power penalties at the receiver, as additional dc power is introduced to protect the useful signal from clipping distortion. However, this tradeoff is beneficial as the effect of modal dispersion is effectively removed.

Assuming the same noise power at the receiver for various dc-biased optical OFDM systems, the minimum required electronic power to achieve certain BERs is compared in Fig. 7. The sufficiently biased OFDM system has the lowest power efficiency, as a very large electronic bias is required. Hence, for illustration purposes, we use it as a baseline and separately normalize the power required by other systems for each individual BER. For the fixed-biased system, with the price of a slightly increased useful signal power (around 0.004), the bias power can be reduced to around 72%, compared to a sufficient-biased system. For the optimally biased system, due to the additional clipping distortion, a much larger useful signal component, typically 1.3–1.7 times stronger, is desired. However, the total electronic power required is the lowest, only 32–39% compared to the sufficiently biased cases.

B. Asymmetrically Clipped Optical OFDM

In Asymmetrically clipped OFDM systems, only limited number of subchannels are loaded with data; some subchannels are reserved to accommodate the clipping distortions. The clipping process also generates an inherent dc term, $E[s_n]$. Therefore, in deriving the effective SNR formulas, we will first adjust QAM symbols so that the OFDM symbol energy is E_s. The effect of the unfavorable dc is then removed when calculating SNR.

1) ACO-OFDM: When I_{DC} in (4) is set to 0, the output distorted signal sequence can also be expressed as

$$s_n = \frac{1}{2}x_n + \frac{1}{2}|x_n| \tag{29}$$

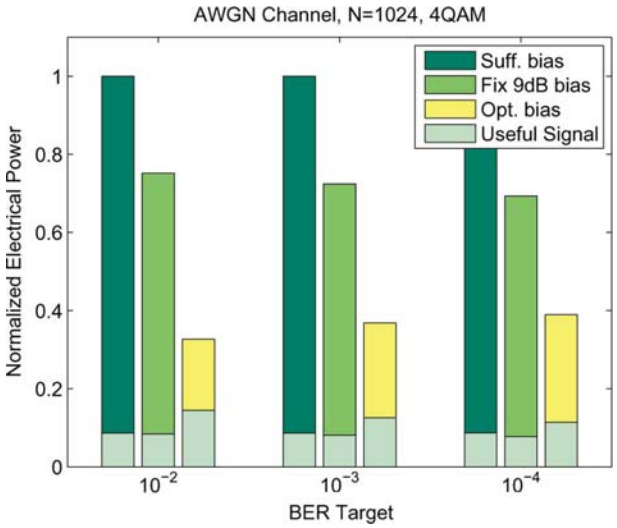

Fig. 7. Minimum electronic power required for different dc-biased optical OFDM to achieve various BER target.

which means that the ACO-OFDM system requires no additional bias because the clipping process itself generates a variable "bias" contained in the second term. It also means that after FFT, half of the received power goes to the odd subchannels, while the other half goes to the clipping distortions on even subchannels. The SNR per received QAM symbol on a data subchannel is then simply

$$\mathrm{SNR_A} = \frac{E_s}{N_0}. \tag{30}$$

2) AC/DC-OFDM: The first term in (29) corresponds to the attenuated signal on the odd subchannels, while the second term is transformed into a noise-like distortion that falls only onto the even subchannels. This natural separation of signal and distortion indicates that if the frequency-domain noise process has relatively low correlations among odd and even subchannels, two highly correlated signals (x_n and $|x_n|$) are virtually delivered through two reasonably independent channels. Hence, in AC/DC-OFDM systems, we have shown that with the help of two additional IFFTs, two estimators of x_n are generated:

$$r_n^{\mathrm{odd}} = \frac{1}{2}x_n + e_n^{\mathrm{odd}}, \quad r_n^{\mathrm{even}} = \frac{1}{2}x_n + e_n^{\mathrm{even}} \tag{31}$$

where the first is the result of a direct IFFT that involves the samples on the odd subchannels only, while the second requires an IFFT of the samples on the even subchannels as well as estimated polarities from the first estimator [29].

The noise processes on these two signals have very different statistical behaviors. e_n^{odd} is a Gaussian process, while e_n^{even} contains both an uncorrelated Gaussian process as well as correlated estimation errors. Note that r_n^{even} is, in general, more noisy than r_n^{odd}. Nevertheless, linearly combining r_n^{odd} and r_n^{even} will still result in a better estimator $\hat{r}_n$, since the signal power is added up coherently while uncorrelated noise is averaged out:

$$\hat{r}_n = (1-\alpha)\, r_n^{\mathrm{odd}} + \alpha\, r_n^{\mathrm{even}} \tag{32}$$

where the combining coefficient α ranges from (0,0.5).

The dependent and impulsive nature of the estimation error e_n^{even} in (31) makes it intractable to evaluate the exact SNR figure of $\hat{r}_n$. However, in a high-SNR region, it is reasonable to model the total noise term inside the r_n^{even} as a Gaussian random process uncorrelated with e_n^{even} and further denote the SNR gap between the two estimators to be η. The SNRs before combining are

$$\mathrm{SNR}^{\mathrm{odd}} = \frac{E_s}{N_0} \quad \text{and} \quad \mathrm{SNR}^{\mathrm{even}} = \eta \cdot \frac{E_s}{N_0}. \tag{33}$$

Under this assumption, the combining coefficients in (32) should be chosen to be linearly proportional to the strength of the signal, i.e., $\alpha/(1-\alpha) = \sqrt{\eta}$. The SNR after combining then achieves its maximum

$$\mathrm{SNR_C} = (1+\eta)\frac{E_s}{N_0}. \tag{34}$$

Since η is smaller than 1, the diversity gain is always smaller than 3 dB.[2] Nevertheless, with simple combining, AC/DC-OFDM system can achieve a lower BER with exactly the same setup for optical transceivers as ACO-OFDM and no additional transmission power.

3) AC/SD-OFDM: In AC/SD-OFDM, a set of antiperiodic signals are created at the transmitter. Asymmetrical clipping of these signals exhibit a similar property as ACO-OFDM whereby nonlinear distortion falls into certain subchannel sets. In other words, the received power on a particular even subchannel could have only a limited, and not necessarily equal, number of sources. Odd subchannels are not affected by any clipping distortion. Therefore, by iteratively characterizing and compensating the clipping distortion, parallel transmission of multiple antiperiodic signals can be achieved.

The electronic driving current of AC/SD-OFDM is the superposition of several asymmetrically clipped anti-periodic signals. For simplicity, we assume here that all subchannels use the same M-QAM constellations with the same energy per symbol.[3] With the help of (14), it is straightforward to derive the effective SNR on the first group

$$\begin{aligned}\mathrm{SNR}^{(1)} &= \frac{\sigma_1^2}{\sum_{i=1}^{u}\sigma_i^2 + 2\sum_{i=1}^{u-1}\sum_{j=i+1}^{u}\frac{\sigma_i\sigma_j}{\pi}} \cdot \frac{E_s}{N_0} \\ &= \frac{1}{2\left(\sum_{i=1}^{u}2^{-i} + \frac{1}{\pi}\sum_{i=1}^{u-1}\sum_{j=i+1}^{u}2^{1-\frac{i+j}{2}}\right)} \cdot \frac{E_s}{N_0}\end{aligned} \tag{35}$$

Due to the nature of soft-decoding, the performance of the later group will be limited by both the receiver noise and the accumulated distortion estimation errors from the previous groups,

[2] η is indeed a function of both the receiver SNR and the modulation format. However, simulation results suggest that, regardless of the correlations, $\eta = 0.75$ and $\alpha = 0.45$ seem to provide a good approximation.

[3] Although in practice, it might be favorable to give more energy or a stronger error protecting code to later groups as they are noisier due to the soft-decoding-based distortion cancellation [29]. A better performance may be achieved by optimizing the power distribution and/or modulation schemes across different signals, but this is outside the scope of this paper and, hence, will not be discussed here.

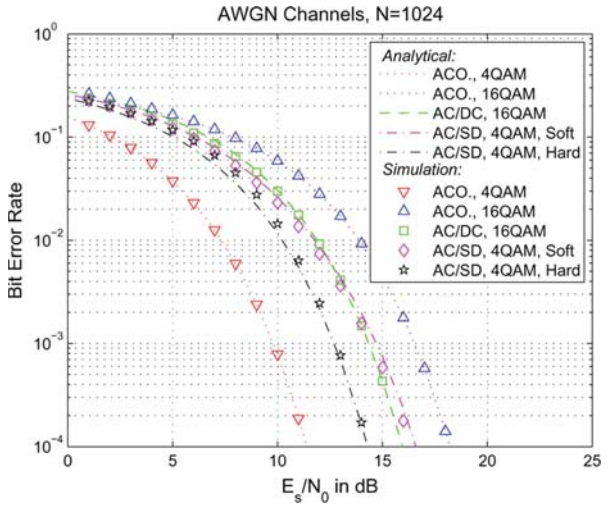

Fig. 8. BER as a function of E_s/N_0 for asymmetrically clipped optical OFDM systems.

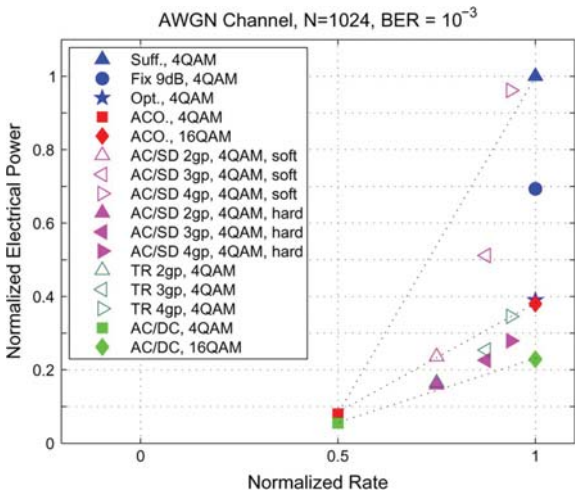

Fig. 9. Normalized electronic power required for a BER of 10^{-3} for various IM/DD optical OFDM systems.

which is roughly a Gaussian process with the variance equals to iN_0. Therefore, the effective SNR for the ith group is then

$$\mathrm{SNR}^{(i)} \approx \frac{1}{i}\mathrm{SNR}^{(1)}. \tag{36}$$

However, when replaced with a hard-decoding-based distortion estimation, the performance of the AC/SD OFDM system could be greatly improved, especially in the high-SNR region, where roughly the same SNR could be obtained across all groups[4]

$$\mathrm{SNR}^{(i)} \approx \mathrm{SNR}^{(1)}. \tag{37}$$

The total BER can then be evaluated by taking a weighted average over all subchannel groups.

Fig. 8 shows the analytical and simulation results for different types of asymmetrically clipped optical OFDM systems, where 1 000 000 random binary bits are again tested in a Monte Carlo setup. In all cases, a very good agreement between the two has been achieved. Since only a quarter of the subchannels can be loaded with data symbols, and with an equal bit-loading across all subchannels, 16-QAM modulation is required for ACO-OFDM and AC/DC-OFDM systems to achieve the same bit rate as 4-QAM dc-biased systems. For AC/SD-OFDM, only two groups of subchannels with 4-QAM are used here. Thus, even though they require less power, the total bit rate is lower than the others.

V. Power Efficiency Discussion

In this section, we analyze the performance of different type of IM/DD optical OFDM systems via Monte-Carlo simulations. All systems have 1024 subchannels, each loaded with 16-QAM complex symbols. 1 000 000 random binary bits are tested and the minimum required power for each system to achieve a BER target of 10^{-3} is compared. The optical attenuation and dispersion is fully compensated so that we can focus on the effect of the bias and clipping. Again, we assume the noise power at the receivers is the same for all systems. For a fair comparison, we further assume that the signal bandwidth for all OFDM systems is limited within the same range. Without loss of generality, both the rate per OFDM symbol and the corresponding power for a sufficiently biased OFDM system are normalized to unity.

Fig. 9 shows the simulation results in terms of electronic power required at the receiver end. We first look at the cases where no further signal processing is employed, i.e., excluding all AC/DC and AC/SD systems. Among dc-biased systems, the optimal-biased strategy provides the best power efficiency by using approximately 36% of the power to achieve the same spectral efficiency. ACO-OFDM is also quite attractive by providing a tradeoff between spectral and power efficiency, where only 8% of the power is required for a half-rate transmission. Full-rate ACO-OFDM requires a slightly higher power than the optimal biased systems and is not preferred as its larger constellation is very vulnerable to beat noise and leftover nonlinear dispersion.

Note that any point along the dashed lines in the figure is achievable, e.g., by using a frequency/time sharing between two schemes. The points below these lines indicate better power efficiencies. If extra complexity and hardware cost can be afforded, more options are available.

With AC/SD systems, it is not efficient to have too many groups. Aside from the increased processing delay and accumulated hardware cost, the power efficiency becomes worse with each additional group. With hard decoding, however, AC/SD is certainly better than ACO-OFDM as both the spectral and power efficiencies are greatly improved. Overall, AC/DC-OFDM is the most power efficient scheme with a power usage of only 5.5% and 23%, for a half-rate and full-rate transmission, respectively. Compared to the ACO-OFDM system and optimal-biased system, a 2.2 dB receiver sensitivity gain can be achieved via diversity combining.

Applying the $\mathbf{P}_o/\mathbf{P}_e$ relationship we developed in Section III, the corresponding optical power required is compared in Fig. 10. The optical power required for dc-biased

[4]Employing hard-decoding-based estimators is not favorable in the very low SNR region, not to mention that it also further increases the system complexity and hardware cost.

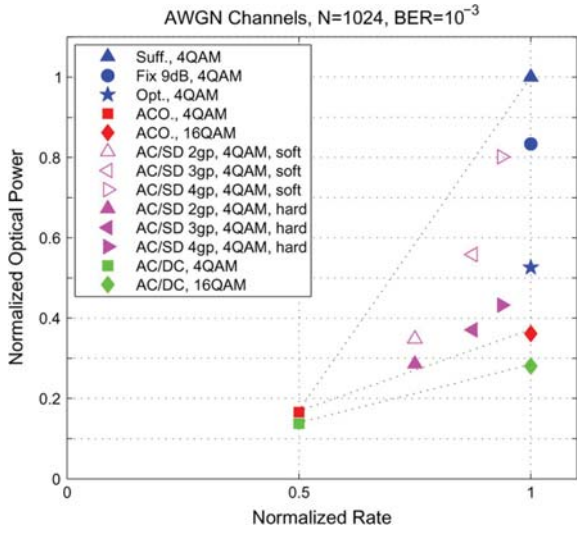

Fig. 10. Normalized optical power required for a BER of 10^{-3} for various IM/DD optical OFDM systems.

systems is significantly higher than for asymmetrically clipped systems due to a larger dc component. The power efficiency of a full-rate, large-constellation ACO-OFDM system stays the same, while the usage for a half-rate ACO-OFDM dramatically increased. As a result, using a smaller constellation but larger bandwidth is no longer power efficient. The AC/SD system also becomes worse due to accumulated dc terms from all its summands. The AC/DC-OFDM system, however, remains the best option by providing a 5.5 dB receiver sensitivity gain over sufficiently biased systems and a 1.1 dB gain over ACO-OFDM systems.

VI. Conclusion

Asymmetric clipping and its associated nonlinear distortion result in a significant performance penalty for OFDM transmissions in IM/DD optical channels. However, we have shown that with a better understanding of its characteristics, such clipping distortion can be optimally controlled, effectively compensated, and even constructively utilized, resulting in an improved power-spectrum tradeoff. In quantifying the power efficiency of a particular IM/DD optical OFDM system, we looked at both the transmission efficiency via $\mathbf{P}_o/\mathbf{P}_e$ and the decoding efficiency via the effective receiver SNR. For low complexity algorithms where clipping distortion is simply treated as noise, an optimally biased system is preferred when electronic power is a cost premium. When optical power is the premium, ACO-OFDM is preferred since it has the lowest detrimental dc component. Furthermore, the distortion power also contains useful information which can easily be extracted by simple diversity-combining method. As a result, AC/DC-OFDM offers a significant performance improvement and is the most efficient modulation scheme in all scenarios.

References

[1] S. Hashemi, Z. Ghassemlooy, L. Chao, and D. Benhaddou, "Orthogonal frequency division multiplexing for indoor optical wireless communications using visible light LEDs," in *Proc. Int. Symp. Commun. Syst. Netw. Digital Signal Process.*, 2008, pp. 174–178.

[2] O. Gonzalez, R. Perez-Jimemnez, S. Rodriguze, J. Rabadan, and A. Ayala, "OFDM over indoor wireless optical channel," *IEE Proc. Optoelectron.*, vol. 152, no. 4, pp. 199–204, 2005.

[3] J. Carruthers and J. Kahn, "Multi-subcarrier modulation for non-directed wireless infrared communication," *IEEE J. Sel. Areas Commun.*, vol. 14, no. 3, pp. 538–546, Apr. 1996.

[4] S. Randel, F. Breyer, and S. C. J. Lee, "High-speed transmission over multimode optical fibers," presented at the presented at the Opt. Fiber Commun. Conf./Nat. Fiber Opt. Eng. Conf., San Diego, CA, 2008, Paper OWR2.

[5] S. Lee, F. Breyer, S. Randel, D. Cardenas, H. van den Boom, and A. Koonen, "Discrete multione modulation for high-speed data transmission over multimode fibers using 850-nm VCSEL," presented at the presented at the Opt. Fiber Commun. Conf./Nat. Fiber Opt. Eng. Conf., San Diego, CA, 2009, Paper OWM2.

[6] I. Djordjevic, B. Vasic, and M. Neifeld, "LDPC-coded OFDM for optical communication systems with direct detection," *IEEE J. Sel. Topics Quantum Electron.*, vol. 13, no. 5, pp. 1446–1454, Sep./Oct. 2007.

[7] J. Tang and K. Shore, "Maximizing the transmission performance of adaptively modulated optical OFDM signals in multimode-fiber link by optimizing analog-to-digital converter," *J. Lightw. Technol.*, vol. 25, no. 3, pp. 787–798, Mar. 2007.

[8] L. Chen, B. Krongold, and J. Evans, "Theoretical Characterization of Nonlinear Clipping Effects in IM/DD Optical OFDM Systems," *IEEE Trans. Commun.*, to be published.

[9] Y. Ma, Y. Tang, and W. Shieh, "107 Gbit/s transmission over multimode fibre with coherent optical OFDM using centre launching technique," *IEE Electron. Lett.*, vol. 45, no. 16, pp. 848–849, 2009.

[10] S. Lee, F. Breyer, S. Randel, O. Ziemannn, H. van den Boom, and A. Koonen, "Low-cost and robust 1-Gbit/s plastic optical fiber link based on light-emitting diode technology," presented at the presented at the Opt. Fiber Commun. Conf./Nat. Fiber Opt. Eng. Conf., San Diego, CA, 2008, Paper OWB3.

[11] S. Lee, F. Breyer, S. Randel, R. Gaudino, G. Bosco, A. Bluschke, M. Mattews, P. Rietzsch, R. Steglich, H. van de Boom, and A. Koonen, "Discrete multitone modulation for maximizing transmission rate in step-index plastic optical fibers," *J. Lightw. Technol.*, vol. 27, no. 11, pp. 1503–1513, Nov. 2009.

[12] H. Yang, S. Lee, E. Tangdiongga, C. Okonkwo, H. van den Boom, F. Breyer, S. Randel, and A. Koonen, "47.7 Gb/s transmission over 100 m graded-index plastic optical fiber based on rate-adaptive discrete multitone modulation," *J. Lightw. Technol.*, vol. 28, no. 4, pp. 352–359, Feb. 2010.

[13] A. Lowery, L. Du, and J. Armstrong, "Performance of optical OFDM in ultralong-haul WDM lightwave systems," *J. Lightw. Technol.*, vol. 25, no. 1, pp. 131–138, Jan. 2007.

[14] W. Shieh and C. Athaudage, "Coherent optical orthogonal frequency division multiplexing," *IEE Electron. Letters*, vol. 42, no. 10, pp. 587–588, 2006.

[15] S. Jansen, I. Morita, T. Schenk, N. Takada, and H. Tanaka, "Coherent optical 25.8-Gb/s OFDM transmission over 4160-km SSMF," *J. Lightw. Technol.*, vol. 26, no. 1, pp. 6–15, Jan. 2008.

[16] B. Schmidt, A. Lowery, and J. Armstrong, "Impact of PMD in single-receiver and polarization-diverse direct-detection optical OFDM," *J. Lightw. Technol.*, vol. 27, no. 14, pp. 2792–2799, Nov. 2009.

[17] Y. Ma, Q. Yang, Y. Tang, S. Chen, and W. Shieh, "1-Tb/s single-channel coherent optical OFDM transmission with orthogonal-band multiplexing and subwavelength bandwidth access," *J. Lightw. Technol.*, vol. 28, no. 4, pp. 308–315, Feb. 2010.

[18] J. Yu, Z. Dong, X. Xiao, Y. Xia, S. Shi, C. Ge, W. Zhou, N. Chi, and Y. Shao, "Generation, transmission and coherent detection of 11.2 Tb/s (112×100 Gb/s) single source optical OFDM superchannel," presented at the presented at the Opt. Fiber Commun. Conf./Nat. Fiber Opt. Eng. Conf., Los Angeles, CA, 2011, Paper PDPA6.

[19] J. Wei, C. Snchez, E. Hugues-Salas, P. Spencer, and J. Tang, "Wavelength-offset filtering in optical OFDM IMDD systems using directly modulated DFB lasers," *J. Lightw. Technol.*, vol. 29, no. 18, pp. 2861–2870, Sep. 2011.

[20] W. Shieh, W. Chen, and R. Tucker, "Polarisation mode dispersion mitigation in coherent optical orthogonal frequency division multiplexed systems," *IEE Electron. Lett.*, vol. 42, no. 17, pp. 996–997, Apr. 2006.

[21] J. Armstrong and A. Lowery, "Power efficient optical OFDM," *IEE Electron. Lett.*, vol. 42, no. 6, pp. 370–372, Mar. 2006.

[22] J. Armstrong, B. Schmidt, D. Kalra, H. Suraweera, and A. Lowery, "Performance of asymmetrically clipped optical OFDM in AWGN for an intensity modulated direct detection system," in *Proc. IEEE Global Commun. Conf.*, 2006.

[23] J. Armstrong and B. Schmidt, "Comparison of asymmetrically clipped optical OFDM and DC-biased optical OFDM in AWGN," *IEEE Commun. Lett.*, vol. 12, no. 5, pp. 343–345, May 2008.
[24] D. Barros and J. Kahn, "OFDM vs. OOK with MLSD for IM/DD systems," presented at the presented at the Opt. Fiber Commun. Conf./Nat. Fiber Opt. Eng. Conf., San Diego, CA, 2010, Paper OThE1.
[25] D. Chanda, A. Sesay, and B. Davies, "Performance of clipped OFDM signal in fiber," in *IEEE Can. Conf. Electr. Comput. Eng.*, May 2004, vol. 4, pp. 2401–2404.
[26] L. Chen, B. Krongold, and J. Evans, "Diversity combining for asymmetrically clipped optical OFDM in IM/DD channels," in *Proc. IEEE Global Commun. Conf.*, 2009.
[27] R. You and J. M. Kahn, "Average power reduction techniques for multiple subcarrier intensity-modulated optical signals," *IEEE Trans. Commun.*, vol. 49, no. 12, pp. 2164–2171, Dec. 2001.
[28] S. Teramoto and T. Ohtsuki, "Multiple-subcarrier optical communication systems with subcarrier signal-point sequence," *IEEE Trans. Commun.*, vol. 53, no. 10, pp. 1738–1743, Oct. 2005.
[29] L. Chen, B. Krongold, and J. Evans, "Successive decoding of anti-periodic OFDM signals in IM/DD optical channel," in *Proc. Int. Conf. Commun.*, 2010, pp. 1–6.
[30] J. Chow, J. Tu, and J. Cioffi, "A discrete multitone transceiver system for HDSL applications," *IEEE J. Sel. Areas Commun.*, vol. 9, no. 6, pp. 895–908, Aug. 1991.
[31] L. Chen, "Distortion management in intensity modulated optical OFDM systems," Ph.D. dissertation, Univ. Melbourne, Australia, 2012.
[32] D. Barros and J. Kahn, "Optical modulator optimization for orthogonal frequency-division multiplexing," *J. Lightw. Technol.*, vol. 27, no. 13, pp. 2370–2378, Jul. 2009.
[33] J. Kahn and J. Barry, "Wireless infrared communications," *Proc. IEEE*, vol. 85, no. 2, pp. 265–298, Feb. 1997.
[34] J. Proakis, *Digital Communications*, 4th ed. New York: McGraw-Hill, 2001.

Liang Chen received the B.E. degree from Zhejiang University, Hangzhou, China, in 2003, and the M.S. degree from the University of Melbourne, Parkville, Vic., Australia, in 2006, where he is currently working toward the Ph.D. degree.

During the winter of 2010, he was a Visiting Researcher at the National Institute of Informatics, Tokyo, Japan. His current research interests include signal processing for both wireless and optical orthogonal frequency-division multiplexing systems.

Mr. Chen was the recipient of Best Paper Awards from the 2006 Australian Communications Theory Workshop and the 2006 European Wireless Conference, respectively. In 2011, he also received a Victoria Fellowship from the Victoria State Government of Australia.

Brian Krongold received the B.S., M.S., and Ph.D. degrees in electrical engineering from the University of Illinois at Urbana-Champaign in 1995, 1997 and 2001, respectively.

He was a Research Assistant at the Coordinated Science Laboratory from 1995 to 2001. From December 2001 to December 2004, he was a Research Fellow in the ARC Special Research Centre for Ultra-Broadband Information Networks in the Department of Electrical and Electronic Engineering, University of Melbourne, Parkville, Vic., Australia, where he has been a Senior Lecturer since January 2008. He was awarded an ARC Postdoctoral Research Fellowship and held this from 2005 to 2008. During the summer of 1994, he interned for Martin Marietta at the Oak Ridge National Laboratory, Oak Ridge, Tennessee. From January to August 1995, he consulted at Bell Laboratories in Middletown, NJ. During the summer of 1998, he was with the Electronics and Telecommunications Research Institute, Taejon, South Korea, under a National Science Foundation summer research grant. During the first half of 2011, he was on sabbatical at Alcatel-Lucent Bell Laboratories in Murray Hill, NJ. His current research interests include multicarrier communications systems, energy-efficient communications, and signal processing for optical communications.

Dr. Krongold received second prize in the Student Paper Contest at the 2001 Asilomar Conference on Signals, Systems, and Computers, and the Best Paper Award at the 2006 European Wireless Conference. His work on active constellation extension for OFDM PAPR reduction is part of the DVB-T2 digital video broadcast standard.

Jamie Evans was born in Newcastle, N.S.W., Australia, in 1970. He received the B.S. degree in physics and the B.E. degree in computer engineering from the University of Newcastle, Newcastle, in 1992 and 1993, respectively. He also received the M.S. and Ph.D. degrees from the University of Melbourne, Parkville, Vic., Australia, in 1996 and 1998, respectively, both in electrical engineering.

From March 1998 to June 1999, he was a Visiting Researcher in the Department of Electrical Engineering and Computer Science, University of California, Berkeley. He returned to Australia to take up a position as Lecturer at the University of Sydney, Sydney, N.S.W., where he stayed until July 2001. Since that time, he has been with the Department of Electrical and Electronic Engineering, University of Melbourne, where he is currently a Professor. His research interests include communications theory, information theory, and statistical signal processing with a focus on wireless communications networks.

Dr. Evans received the University Medal upon graduation from the University of Newcastle. He received the Chancellor's Prize for excellence for his Ph.D. dissertation.